NANOCRYSTALS OF NATIVE MOLYBDENUM, IRON AND TITANIUM WITHIN IMPACT GLASSES OF LUNAR REGOLITH

Andrey V. Mokhov, Tatyana A. Gornostaeva, Pavel M. Kartashov, Enver E. Asadulin, Oleg A. Bogatikov

Institute of Geology of Ore Deposits, Petrography, Mineralogy and Geochemistry (IGEM), Russian Academy of Sciences, Moscow, avm@igem.ru

This paper discusses the results of study of the impact glass fragments from the Mare Fecunditatis and Mare Crisium regolith samples brought on the Earth by the Soviet Automatic stations Luna-16 and Luna-24. Nanoinclusions of native molybdenum, iron and titanium were found in the samples with scanning and transmission electron microscopy (SEM, TEM). It is shown that these inclusions are single crystals. A natural high pressure native ω-titanium was identified for the first time. The composition and structure of glass matrix of the regolith samples indicates its extreme micro and nano heterogeneity. The probable formation mechanisms of the studied nanocrystals are discussed.

3 tables, 10 figures, 26 references.

Keywords: native molybdenum, native iron, native ω-titanium, nanophases, single crystals, impact glasses, lunar regolith, Mare Fecunditatis, Mare Crisium.

The main goal of the investigation of minerals from lunar regolith (average fine lunar matter) was detetermination of the composition and structure of microphases reflecting specific character of mineral-forming processes at high temperature and pressure gradient in oxygen-free and anhydrous atmosphere. The impact events determining chemical and physical properties of lunar regolith made a substantial contribution to the formation of these phases. However, large grains of native metals have not been found on the Moon yet. These are fine particles up to 150 μm in size (Frondel, 1975), that predetermined methods of our study.

Particularly, native molybdenum as thin films and spherical submicron grains was frequently found in the Mare Fecunditatis and Mare Crisium regolith samples studying with SEM (Bogatikov *et al.*, 2001; Mokhov *et al.*, 2007; Kartashov *et al.*, 2010).

Iron is the most abundant metal on the Moon; it occurs as oxidized and native species (Frondel, 1975). Irregular-shaped, ribbon-like, spherical, and drop-like particles of native iron are the most abundant in lunar regolith (Mokhov *et al.*, 2007).

Nonvalent iron, aluminum, silicon and titanium were identified with the X-ray photo electron spectroscopy studying condensate glass film coating the lunar regolith samples from the Mare Fecunditatis (Yakovlev *et al.*, 2009). However, these data only indirectly verify metallic titanium in lunar glass and do not provide reliable information on its structure.

Therefore, the aim of this study is investigation of structure and formation mechanisms of metal inclusions in lunar glasses.

Analytical techniques

Glass fragments of the regolith samples from the Mare Fecunditatis and Mare Crisium brought to the Earth by AS Luna-16 and Luna-24 were examined with transmission (TEM) and scanning (SEM) analytical electron microscopy using a JEM-2100 microscope equipped with an IETEM spectrometer INCA-250 and a JSM-5610LV scanning electron microscope equipped with an INCA-450 EDS.

Supporting of purity and prevention of contamination by foreign phases has been regarded in the preparation of fine-dispersed samples of lunar glasses for the SEM analysis. A conductive double-sided tape in whose composition only carbon and oxygen were detected (within detection limits of EDS) was stuck on ordinary aluminum tables. A tape-free surface of the table was coated with graphite glue to avoid a fluorescence of aluminum. Immediately after opening, regolith sample was spread as a thin layer on the inner side of the tape with removed protective film and the table with the prepared sample was enclosed in clear Petri dish and was placed in a special storage till the start of electron microscopic study. Thus, a contamination of sample by artifacts is eliminated as far as possible. Minerals and metals already

Table 1. **Compositions of glasses and pyroxene (wt.%) in samples of studied lunar regolith**

Analysis	1	2	3*	4	5	6	7	8
Na_2O	3.9±0.5	2.3±0.4	–	–	–	4.2±0.5	1.4±0.4	–
MgO	1.3±0.2	2.3±0.2	6.7±0.3	14.8±0.3	4.9±0.3	2.7±0.3	–	6.21±0.3
Al_2O_3	7.3±0.3	24.5±0.5	18.0±0.4	–	13.0±0.4	22.8±0.5	25.6±0.6	13.6±0.4
SiO_2	53.9±0.5	58.1±0.7	43.2±0.6	51.9±0.7	36.7±0.5	54.0±0.8	61.7±0.8	42.4±0.6
K_2O	–	–	–	–	0.3±0.2	3.7±0.6	–	–
CaO	5.8±0.2	5.2±0.3	14.6±0.4	8.2±0.3	17.4±0.4	–	11.3±0.4	14.4±0.4
TiO_2	0.9±0.1	–	–	–	5.6±0.3	–	–	4.2±0.2
FeO	26.8±0.5	5.1±0.3	17.1±0.5	25.1±0.4	22.1±0.6	12.6±0.5	–	19.1±0.4
BaO	–	2.6±0.4	–	–	–	–	–	–

*Notes: Total is normalized to 100%. *– Contents of Na_2O, K_2O, and Cl below 0.2 wt.%. Analysts A.V. Mokhov and T.A. Gornostaeva.*

analyzed were prepared according to the procedure of Lapina and Mokhov (1995) for using as reference samples.

A possible contamination of the samples with foreign matter is the most dangerous in these studies and put in question these findings. It refers first of all to micro and nanoparticles, which could easily contaminate a sample. We confidently can state that the phases studied are not impurities only if they were coated with glass or shallowly sank into it. Frequently, these phases are sufficiently contrasted to be detected because back-scattered electrons are generated and drift out of the sample from the relatively great depth. To demonstrate that the particles are coated with glass layer an imaging in secondary electrons is used because these electrons drift out of the sample from quite shallow depth and allow obtaining information of the morphological features of the sample regardless its mean atomic weight.

Samples were prepared for TEM according to suspension method of Gritsaenko (1969). This method is the most common because it is very informative and simple. A glass fragment nearly hundred microns or larger in size was placed into clear test microtube. Then, the test tube with a piece of glass in few amount of distil analytically pure water was placed into sonicator for disintegration. A sample crushed by ultrasound in water drop was placed on a special cooper grid with film of formovar and collodion and then was dried at 35°C in drying box.

Results

As a result of the SEM study massive spherules of native molybdenum (Fig. 1) were identified in glass of the Mare Crisium regolith samples with average composition given in Table 1 (an. 1). Secondary and back-scattered electron images (Figs. 1a, 1b) clearly show a glass coating that eliminates contamination of sample by man-made molybdenum. However, because of glass coating, the identified inclusions did not show electron backscattered diffraction (EBSD) patterns. These patterns (Fig. 2) supporting metallic state of molybdenum grains (Table 2) were obtained only after ion beam cutting of the glass coat.

Nanocrystals of native molybdenum (Fig. 3), which occur as chains to form trichoid structures (Fig. 4) in glass or as massive segregations also in glass (Fig. 5) were identified as a result of the TEM study. In the first case, the microdiffraction patterns show low intensive discrete-ring reflections of native molybdenum, whereas in the second case, the microdiffraction patterns are absent because of great thickness of the samples. The composition of glass is close to that determined with SEM (Table 1, an. 1), however, the higher content of silica, much lower concentration of Fe, and small amount of Ba were measured (Table 1, an. 2).

Numerous micro- and nanoinclusions of native iron were found in the Mare Fecunditatis glass samples with SEM and TEM. Matrix glass containing these inclusions inhomogeneous even in scanning electron microscope is moreover inhomogeneous in transmission electron microscope with the composition significantly different from that determined with SEM (Table 1, an. 3). Numerous fragments of this glass contain both spherical nanoparticles and larger irregular-shaped particles. Point TEM analysis showed that these larger irregular-shaped microinclusions are different in composition corresponding to the rock-forming silicates (plagioclase, pyroxene, olivine), whereas nanoin-

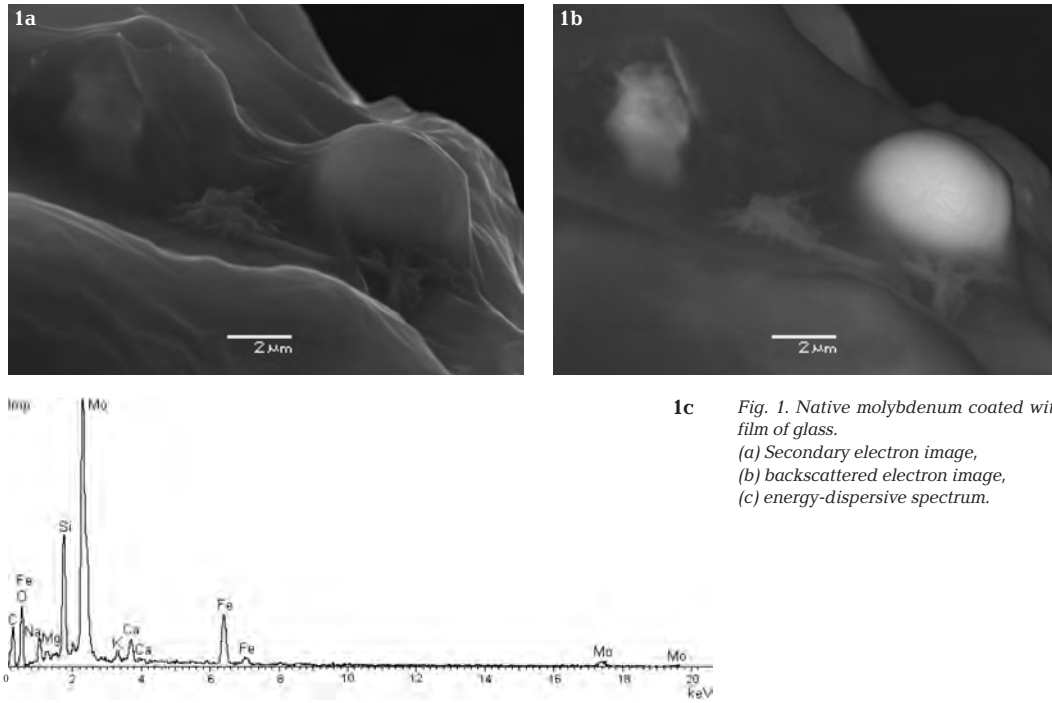

1c

Fig. 1. Native molybdenum coated with film of glass.
(a) Secondary electron image,
(b) backscattered electron image,
(c) energy-dispersive spectrum.

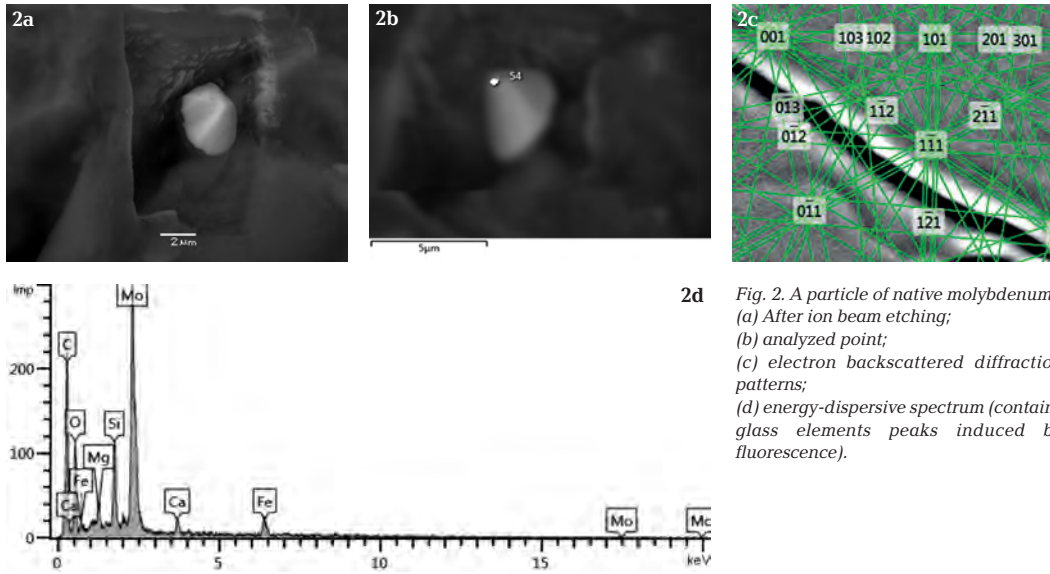

2d

Fig. 2. A particle of native molybdenum.
(a) After ion beam etching;
(b) analyzed point;
(c) electron backscattered diffraction patterns;
(d) energy-dispersive spectrum (contains glass elements peaks induced by fluorescence).

clusions are enriched only in Fe in comparison with glass.

Figure 6 shows the glass fragment containing large irregular-shaped inclusion whose composition given in Table 1 (an. 4) corresponds to pigeonite $(Mg_{0.85}Fe_{0.81}Ca_{0.34})_2(Si_2O_6)$, In addition, many spherical nanoinclusions are shown in Fig. 6. The elemental distribution patterns within one of the glass fragments containing the largest inclusions of this type were obtained to determine the exact composition of these globules. The patterns obtained verified an absence of oxygen and appreciable contents of other elements than iron in globules. The microdiffraction pattern registered for such globule contained weak reflections *110* of cubic native α-iron with *a* of 0.28 nm and space group *Im*-3*m*.

High resolution imaging revealed a periodicity of structure with step of 0.2 nm that corresponds to *d*-spacing characteristic of this type reflections (Fig. 7).

The irregular-shaped inclusions of native titanium (Fig. 8a) of a few to a few tens nanometers in size were found in a glass fragment similar to titanaugite in composition (Table 1, an. 5). The microdiffraction patterns confirmed that native titanium is high-pressure hexagonal ω-modification with *a* 0.462 nm and space group *P*6/*mmm*. Fig. 8b shows the microdiffraction pattern of this phase in plane (*001*). The diffraction modeling of the structure of the native titanium ω-modification using the eMap software package supported the identity of model obtained and microdiffraction pattern.

High resolution imaging has identified *hk*0 type planes of native titanium with 2D picture with *d*-spacing 0.23 nm corresponding to *11.0* reflections being recorded in one case. In the other cases, only 1D structure has been displayed because of inexact match of structural planes with transmitting electron beam.

It should be noted that glass fragments in the Mare Fecunditatis and Mare Crisium samples are remarkably variable in compositions as it follows from the high resolution measurements. It is the most pronounced in TEM with resolution of 5 to 10 nm. Glasses close in composition to silicate phases are frequent. For example, the glass fragments with the compositions satisfactorily recalculated on formulas of sodium feldspar, olivine and pyroxenes were found. Also a few fragments of Si-rich glasses containing only 2−7 wt.% Al_2O_3 in addition to SiO_2. Heterogeneity of glasses was presented even at nanoscale level.

Table 2. **Result of automatic identification of phase according to the EBSD data based on Inorganic Crystal Structure Database**

Name	**Mo**
Symmetry	Cubic
Laue class	11
Space group	*Im*-3*m* (229)
Unit cell	
a	3.15 Å
b	3.15 Å
c	3.15 Å
α	90.00°
β	90.00°
γ	90.00°

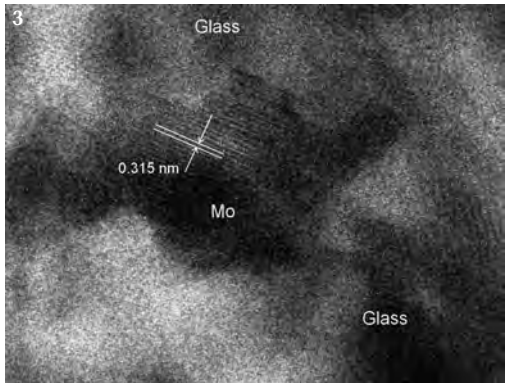

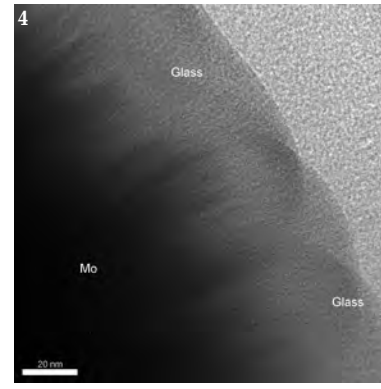

Fig. 3. Transmission electron microscopy image of native molybdenum nanocrystal in glass.

Fig. 4. Transmission electron microscopy image of native molybdenum coated with glass layer.

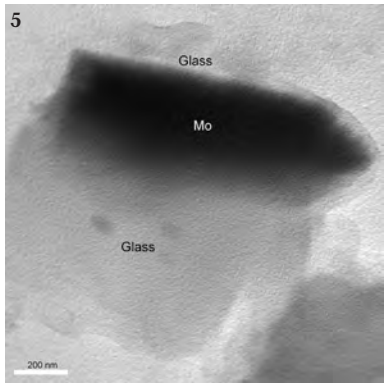

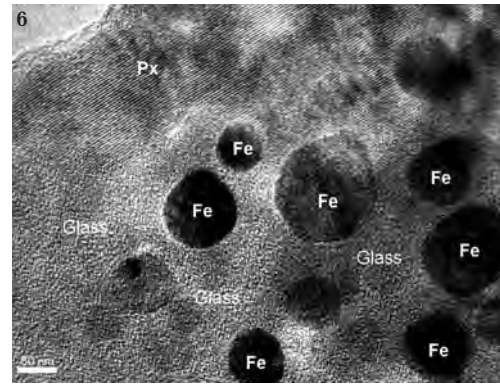

Fig. 5. Transmission electron microscopy image of aggregate of native molybdenum coated with glass layer.

Fig. 6. Transmission electron microscopy image of glass of the AS "Luna-16" regolith with inclusions of iron spherules and pyroxene.

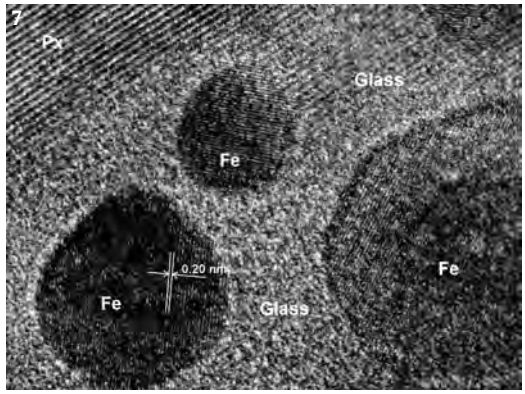

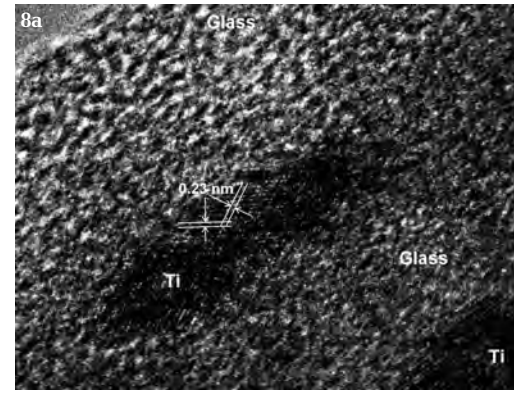

Fig. 7. Transmission electron microscopy image of single crystal spherules of native iron.

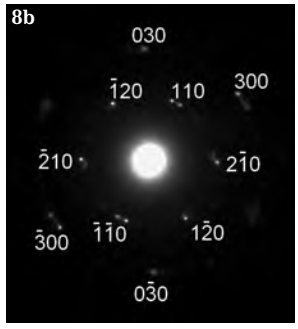

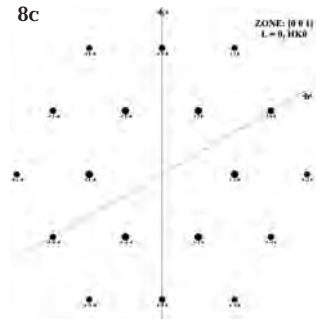

Fig. 8. Single crystal grains of native ω-Ti in pyroxene glass.
(a) Transmission electron microscopy image of separate nanocrystal of native ω-Ti;
(b) its microdiffraction pattern;
(c) model developed in eMap.

For example the structure of pyroxene composition glass is heterogeneous in size and distribution of structural clusters. The fragment of glass tough and homogeneous in the core is characterized by larger disordered clusters in the rim. The composition of this external unconsolidated glass film (Table 1, an. 6) substantially differs from that of matrix (Table 1, an. 5).

Thin glass layer of 5 to 30 nm thick different in composition from matrix is frequently observed on the TEM images. It coats as hardly distinguishable layer both mineral phases of different composition and other glasses. Native molybdenum in such glass is shown in Fig. 4 and a thin glass layer of other density (Table 1, an. 7) coating massive glass (Table 1, an. 8) similar to that shown in Fig. 8a is seen in Fig. 9.

Coating glasses are variable in composition that differs from that of matrix both quantitative and quailitative. In particular, barium traces were measured in glass coating native molybdenum and small sodium peaks were recorded in glass coating native iron and titanium.

Of special note are high resolution images of glass coating native iron, molybdenum and titanium demonstrating single crystal and nano-sized character of their grains.

Discussion

It should be noted that native molybdenum has been previously found with SEM by Bogatikov *et al.* (2001) and Kartashov *et al.* (2010), but no any structure characteristics were obtained. Currently, as a result of the EBSD and TEM study, not only native state of molybdenum was confirmed, but its formation as aggregates of nano-sized single crystsls was established. In other words, the distinction of lunar molybdenum crystallized in the cubic system from hexamolybdenum phase discovered in C chondrites (Ma *et al.*, 2009) not only in composition, but in structure was confirmed. Native molybdenum was found on the Earth as an inclusion in carbonado (Silaev *et al.*, 2004) although no structural data were given.

As a result of previous TEM study of lunar glasses, nanoinclusions of iron ranging from a few to a few hundreds nm in size were found (James *et al.*, 2002). These iron-bearing inclusions were interpreted as native iron, but reliable evidences about presence of these particles as metallic species were not reported. We did not find any information on the crystallinity degree of these grains (Keller, McKay, 1993; Thompson, Christoffersen, 2010). However, now we have established

monocrystalline character of these nanograins.

Nonvalent titanium has been identified in glasses of the Moon studied with X-ray photoelectronic spectroscopy (Dickov *et al.*, 1977; Yakovlev *et al.*, 2009). Native titanium was found on the Earth many times. For the first time it was mentioned by Trunilina *et al.* (1988), who reported the millimeter-size lamellae of native titanium in crushed leucogranite samples from the Bezhymyannyi Pluton in the northeastern Yakutia. Then titanium as micrograins in association with other native metals, carbides and carbons was found in fumarole exhalations of The Great Tolbachik Fissure Eruption occurred in 1975 (Glavatskikh and Gorshkov, 1992). In the last case, its structural parameters were determined with electron microdiffraction. This proved an existence of titanium as α-species and polycrystalline nature of found aggregate. The resolution of used transmission electron microscope was insufficient for determination of size and shape of single crystals in these aggregates.

Finally, native titanium was approved as mineral species on material from the Luobusha chromite massif in Tibet (Fang *et al.*, 2013), where it is associated with native metals, intermetallic compounds, alloys, diamonds, and various carbides and silicides. Associations and direct intergrowths of titanium with the high-pressure phases allowed estimating pressure range of 2.8 to 4 GPa under which it can be formed. Nevertheless, a common low-pressure α-titanium with $P6_3/mmc$ space group was found there (Fang *et al.*, 2013).

We identified natural high-pressure ω-titanium polymorph with $P6/mmc$ space group for the first time. According to Jamieson (1963), α-titanium transits to ω-species at 6 GPa.

How do we explain the presence α-titanium the high-pressure mantle assemblage in Tibet? The answer is found in the same paper by Jamieson (1963). Annealing of ω-titanium at 110°C for 17 h causes transition of ω- to α-modification. Obviously, initially high pressure ω-titanium transited to α-modification as a result of retrograde metamorphism of host chromitite in the upper crust. At the same time, lunar ω-titanium resulted from high-energy impact event (possibly during the formation of diaplectic glass after titanaugite crystal) was quickly quenched owing to rapidity of an impact process. Indeed, colossal PT values exists only during

Fig. 9. Transmission electron microscopy image of glass coated with thin layer of another glass.

microseconds at impact. Apparently, the sample studied was not annealed after being formed and quenched and it was preserved in initial state in glass to recent time.

In general, the data obtained indicate a significant heterogeneity of low-Si matrix glasses. Frikh-Khar *et al.* (1988) were the first who noticed heterogeneity of lunar glasses at submicron level studying with scanning electron microscope. The compositional heterogeneity of glasses from regolith samples collected in area of AS Luna-16 landing have been earlier detected by Dikov *et al.* (1998, 2002) using layer by layer analysis performed with X-ray photoelectron spectroscopy. As a result, variable compositions both between layers and within individual layer in lateral direction were established. The Na-rich nano-size coarse-cluster layer of glass could be explained by vapor condensation out of impact cloud. The fragments of more refractory high-Si glass consolidating before low-Si glass are emplaced into liquid low-Si matrix

Table 3. **Minimum value (min), median (Me), arithmetical mean (m), maximum value (max) of component contents in glasses**

Components, wt.%	min	Me	m	max	n*
SiO_2	30.71	54.39	63.84	97.67	78
TiO_2	0.05	0.68	0.84	5.86	34
Al_2O_3	0.96	4.50	8.88	34.08	77
FeO	0.06	13.37	12.81	35.35	55
MgO	0.05	5.39	6.63	32.40	61
CaO	0.15	6.45	7.14	25.83	73
Na_2O	0.09	1.62	3.78	25.41	55
K_2O	0.13	0.49	1.53	8.27	42

*Notes: * — 78 observations in total, n — denotes number of observations with the component content higher above detection limit.*

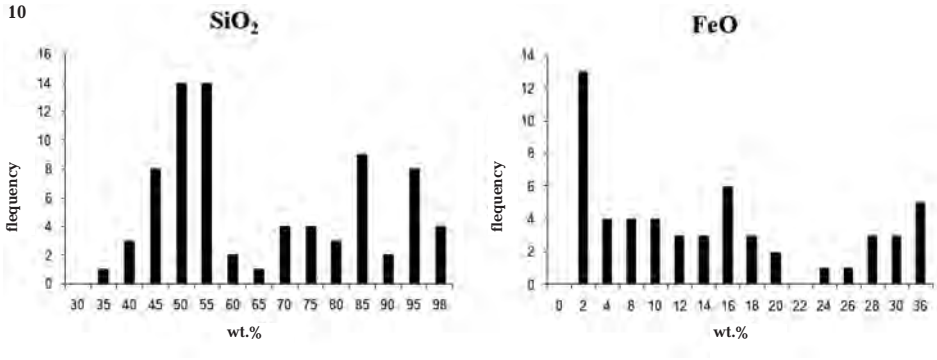

Fig. 10. Histograms of SiO_2 and FeO contents obtained studying lunar regolith glasses with high resolution.

as solids. Microfragments of diaplectic glasses are also emplaced in it. In addition, nanoparticles of some mineral (crystalline) phases were emplaced into studied low-Si glass. Thus, a few versions regard to the origin of native iron inclusions in glass are suggested. Two mechanisms are believed to be major.

According to the first, the drops of native iron resulted from impact and immediately crystallized were emplaced into liquid glass. This mechanism is supported by the presence of large pyroxene single crystal probably raised up from the surface as a result of explosion and trapped by the glass. Apparently, this mechanism explains the presence of molybdenum nanocrystalls and other mineral phases in glass (Mokhov *et al.*, 2007; Kartashov *et al.*, 2010; Mokhov *et al.*, 2011; Gornostaeva *et al.*, 2012).

According to the second mechanism that is very popular among researchers, Fe^0 is resulted from impact melting and reduction of silicate Fe^{2+} as affected hydrogen implanted by solar wind (Housley *et al.*, 1973; Wang *et al.*, 2012).

Massive (exceeding a few unit cells in volume) particles of native iron are thought to be unlikely resulted from disproportionate reaction in impact cloud (Yakovlev *et al.*, 2009).

The data of high-resolution elemental analysis obtained with SEM and TEM were processed to estimate a degree of homogeneity of glass. Only values higher than detection limits were taken into account; therefore, numbers of element measurements are different. Results are given in Table 3 as follows: minimum value, median, arithmetical mean (AM), maximum value, and number of observations. Dispersion between minimum and maximum concentration along with differences in median values and arithmetical means indicate heterogeneity of the material. Histograms demonstrate this vividly. For example, Fig. 10 shows histograms of SiO_2 and FeO contents which exceed 60% of in the chemical composition of the glasses examined. Multimodal distribution of these constituents indicates quite obviously heterogeneity of the material studied.

Of special note is the isolating role of glass or more likely condensate film coating nearly all mineral microparticles with nanosize layer in the studied regolith samples and preventing native phases from oxidation and interaction with other phases.

Conclusions

1. Aforementioned native metals are nanocrystals or aggregates of nanocrystals implying short period of crystallization. This corresponds conditions of impact events on the Moon.

2. The presence of glasses dramatically different in composition, physical properties (particularly in melt temperature and fugacity of constituents), and structure of their aggregates in the same regolith particle allows to assume significant difference in the energy range of impact events, which caused their formation. In other words, regolith samples studied are a product of multiple impacts with different energy, i.e. with different masses and velocities of impactors.

3. Both native metals and many other mineral phases in the samples studied are usually coated with thin sometimes nano-thick condensate films of glass. It supports an authenticity of these inclusions and explains the inoxidability of lunar native iron (probably also other minerals) in the Earth environment conditions that is alternative to explanation of inoxidability caused by long bombardment by protons of solar wind (Vinogradov *et al.*, 1972; Vinogradov *et al.*, 1979).

Acknowledgements

This study was supported by the Russian Foundation for Basic Research (project no. 12-05-00624a).

References

Bogatikov O.A., Gorshkov A.I., Mokhov A.V., Ashikhmina N.A., Magazina L.O. The first finding of native molybdenum, silver sulphide and iron-tin alloy in the lunar regolith // Geochem. Int. **2001**. Vol. 39. No. 6. P. 604–608.

Dikov Yu.P., Nemoshkalenko V.V. Aleshin V.G. Bogatikov O.A., Ivanov A.V. Reduce titanium in lunar regolith // Dokl. Acad. Nauk SSSR. **1977**. Vol. 234. No. 1. P. 176–179 (in Russian).

Dikov Yu.P., Ivanov A.V., Wlotzka F., Galimov E.M., Wanke G. High enrichment of carbon and volatile elements in the surface layers of Lunar 16 soil sample 1635: results of comet or meteorite impact? // Earth Planet. Sci. Lett. **1998**. Vol. 155. P. 197–204.

Dikov Yu.P., Ivanov A.V., Wlotzka F., Galimov E.M., Wanke G. The nature of volatiles in the lunar regolith // Solar System Research. January **2002**. Vol. 36. Issue 1. P. 1–11.

Fang Q., Bai W., Yang J., Rong H., Shi N., Li G., Xiong M., Ma Z. Titanium, Ti, a new mineral species from Luobusha, Tibet, China // Acta Geol. Sinica. **2013**. Vol. 87. No. 5. P. 1275–1280.

Frikh-Khar D.I., Boyarskaya R.V., Volkova V.M., Kostin K.B., Mokhov A.V. Inhomogeneity in natural glasses // Int. Geol. Rev. **1988**. Vol. 30. No. 4. P. 422–429.

Frondel J.W. Lunar Mineralogy. New York: Wiley-Interscience. **1975**. 332 p.

Glavatskih S.F., Gorshkov A.I. Natural analog of α-titanium in exhalations of The Great Tolbachik Fissure Eruption (Kamchatka) // Dokl. Acad. Nauk. **1992**. Vol. 327. No. 1. P. 126–130 (in Russian).

Gornostaeva T.A., Kartashov P.M., Mokhov A.V., Bogatikov O.A. Native rhodium-bearing ferroplatinum in a lunar regolith sample from the Mare Fecunditatis // Dokl. Earth Sci. **2012**. Vol. 444. No. 2. P. 770–772.

Gritsaenko G.S., Zvyagin B.B., Boyarskaya R.V., Gorshkov A.I, Samotoin N.D., Frolova K.E. Methods of electron microscopy of minerals. Moscow: Nauka. **1969**. 311 p. (in Russian).

Housley R.M., Grant R.W., Paton N.E. Origin and characteristics of excess Fe metal in lunar glass welded aggregates // Proc. of the Fourth Lunar Sci. Conf. Suppl. No 4. Geochim. et Cosmochm. Acta. **1973**. Vol. 3. P. 2737–2749.

James C., Letsinger S., Basu A., Wentworth S.J., McKay D.S. Size distribution of Fe^0 globules in lunar agglutinitic glass // 33nd Lunar and Planetary Sci. Conf. Houston, Texas. **2002**. (abstract #1827). CD-ROM.

Jamieson J.C. Crystal structures of titanium, zirconium and hafnium at high pressures // Science. **1963**. Vol. 140. No. 3562. P. 72–73.

Kartashov P.M., Mokhov A.V., Gornostaeva T.A., Bogatikov O.A., Ashikhmina N.A. Mineral phases on the fracture of a glass particle and in the fines of a Luna 24 regolith sample // Petrology. **2010**. Vol. 18. No. 2. P. 107–125.

Keller L.P., McKay D.S. Discovery of vapor deposits in the lunar regolith // Science. **1993**. Vol. 261. P. 1305–1307.

Lapina M.I., Mokhov A.V. Technique of reference samples preparation for transmission, scanning electron microscopy and microprobe analysis // Bull. Russian Acad. Sci., Ser. Physics. **1995**. Vol. 59. No. 2. P. 38–41 (in Russian).

Ma C., Beckett J.R., Rossman G.R. Allendeite and hexamolybdenum: two new ultra-refractory minerals in Allende and two missing links // 40th Lunar and Planetary Sci. Conf. Houston, Texas. **2009**. P. 1402–1403.

Mokhov A.V., Kartashov P.M., Bogatikov O.A. New data on mineralogy of the Moon (the Moon under microscope) // Ed. Bortnikov N.S. Moscow: Nauka. **2007**. 128 p. (in Russian).

Mokhov A.V., Kartashov P.M., Gornostaeva T.A., Bogatikov O.A. Native ytterbium of AS Luna-24 regolith // Dokl. Earth. Sci. **2011**. Vol. 441. No. 2. P. 1692–1694.

Silaev V.I., Petrovsky V.A., Sukharev A.E., Martins M. Carbonado: a brief review of examination // Bull. Inst. Geol. Komi Sci. Center, Urall Branch, Russian Academy of Sciences. **2004**. No. 11. P. 7–13 (in Russian).

Thompson M., Christoffersen R. The smallest lunar grains: analytical tem characterization of the sub-micron size fraction of a mare soil // 41st Lunar and Planetary Sci. Conf. Houston, Texas. **2010**. P. 2191.

Trunilina V.A., Roev S.P., Makhotko V.F., Zayakina N.B. Native titanium in granitiods of the Bezymyany Pluton, East Yakutia // Dokl. Acad. Nauk SSSR. **1988**. Vol. 303. No. 4. P. 948–951 (in Russian).

Vinogradov A.P., Barsukov V.L., Urusov V.S., Bogatikov O.A. Unoxidability feature of

ultradisperse species of elements existing on the surface of space bodies // Find certificate No 279 registered in National find registry of the USSR November, 15. **1979** (in Russian).

Vinogradov A.P., Nefedov V.I., Urusov V.S., Zhavoronkov N.M. X-ray photoelectron study of metallic iron in lunar regolith // Dokl. Acad. Nauk SSSR. **1972**. Vol. 207. No. 4. P. 433–436 (in Russian).

Wang K., Moynier F., Podosek F.A., Foriel J. An iron isotope perspective on the origin of the nanophase metallic iron in lunar regolith // Earth Planetary Sci. Lett. **2012**. Vol. 337–338. P. 17–24.

Yakovlev O.I., Dikov Yu.P., Gerasimov M.B. Effect of the disproportionation reaction of ferrous iron in impact-evaporation processes // Geochem. Int. **2009**. Vol. 47. No. 2. P. 134–142.